Journal of Achievements in Materials and Manufacturing Engineering
VOLUME 38
ISSUE 1
January
2010

Influence of nickel on structure and hardness of Fe-Co bulk metallic glasses

R. Nowosielski, A. Januszka*
Division of Nanocrystalline and Functional Materials and Sustainable Pro-ecological Technologies, Institute of Engineering Materials and Biomaterials,
Silesian University of Technology, ul. Konarskiego 18a, 44-100 Gliwice, Poland
* Corresponding author: E-mail address: anna.januszka@polsl.pl

Received 15.11.2009; published in revised form 01.01.2010

Materials

ABSTRACT

Purpose: In the present paper, influence of Ni addition on structure and hardness Fe-based bulk metallic glass were investigated.
Design/methodology/approach: The studies were performed on $Fe_{36+x}Co_{36-x-y}Ni_yB_{19.2}Si_{4.8}Nb_4$ (x= 0;1, y=0;10;15) glassy alloy in a form of rods with diameter up to 5 mm. The tests, carried out to obtain amorphous metallic glasses, were realized with the use pressure die casting method. The system includes a copper mould, high frequency power supply, quartz nozzle and a source of inert gas as argon. The following experimental techniques were used for the test of structure: X-ray diffraction (XRD) phase analysis and scanning electron microscopy (SEM). Microhardness was examined by Vickers diamond testing machine.
Findings: The X-ray diffraction revealed that all samples with thickness 2 mm were amorphous. The structural studies revealed that amorphous structure depended on thickness and nickel contents in a preliminary alloy.
Research limitations/implications: The relationship between structure and microhardness can be useful for practical application of these alloys.
Practical implications: The Fe-based bulk metallic glasses attracted great interest for a variety of application fields, for example structural materials, electric applications, precision machinery materials. These amorphous alloys exhibit high strength, a high elastic strain limit, high fracture toughness, and other useful mechanical properties which are attractive to many engineering applications.
Originality/value: The originality of this paper are studies of changes of structure and hardness of $Fe_{36+x}Co_{36-x-y}NiyB_{19.2}Si_{4.8}Nb_4$ (x= 0;1, y=0;10;15) mainly depending on Ni addition in this alloy.
Keywords: Bulk metallic glasses; Amorphous materials; Die casting; Glass Forming Ability; Mechanical properties

Reference to this paper should be given in the following way:
R. Nowosielski, A. Januszka, Influence of nickel on structure and hardness of Fe-Co bulk metallic glasses, Journal of Achievements in Materials and Manufacturing Engineering 38/1 (2010) 15-23.

1. Introduction

Metallic glasses (also known as metallic amorphous alloys) are newcomers to the group of amorphous materials. First, metallic glass ($Au_{75}Si_{25}$) was made by Duwez in 1960 and developed with the use of the rapid quenched techniques for chilling metallic liquids [1, 2]. Metallic glasses are interesting materials because of their scientific importance and potential engineering application. Melt quenching techniques are still extensively developed and elaborated to produce various metallic glasses. Chen in 1974 prepared first „bulk" metallic glass – ternary Pd-Cu-Si alloy (millimetre-diameter rods) made in simple suction-casting methods. Next successful attempt was made in

1982 – Turnbull and co-workers successfully prepared Pd-Ni-P bulk metallic glass by using boron oxide fixing method. From early 1980s bulk metallic glasses were made with completely different mechanism from rapid quenching: die casting, centrifugal casting, or suction casting. Fig. 1 shows the critical casting thickness for some bulk metallic glasses as a function of their year of discovery [3, 4, 5, 6].

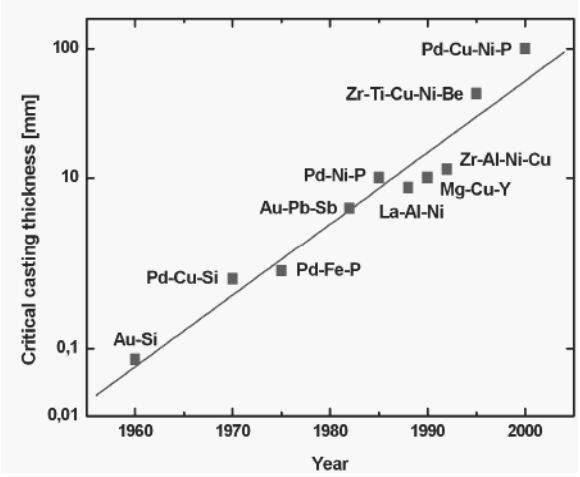

Fig. 1. Relationship between the critical casting thickness and the year of discovery of some bulk metallic glasses [1]

Table 1.
Characteristic indicators for GFA definition [10, 11]

GFA indicators	Expression	Year established
T_{rg}	$\frac{T_g}{T_l}, \frac{T_g}{T_m}$	1969, 2000
K_{gl}	$\frac{T_x - T_g}{T_m - T_x}$	1972
ΔT_{xg}	$T_x - T_g$	1993
γ	$\frac{T_x}{T_g + T_l}$	2002
δ	$\frac{T_x}{T_l - T_g}$	2005
α	$\frac{T_x}{T_l} = \frac{\Delta T_{xg}}{T_l} + \frac{T_g}{T_l}$	2005
β	$\frac{T_x}{T_g} + \frac{T_g}{T_l} \approx \frac{T_x}{T_g} + 1$	2005
ξ	$\frac{\Delta T_{xg}}{T_x} + \frac{T_g}{T_l}$	2008
β	$\left(\frac{T_g}{T_l - T_g}\right) \cdot \left(\frac{T_x}{T_l - T_g}\right)$	2008

Since the first Fe-based ferromagnetic bulk metallic glass in an Fe(Al,Ga)-metalloid alloy system was developed in 1995 a variety of Fe-based BMGs have been synthesized which can be generally classified by two groups: non-ferromagnetic (such as Fe-Mn-Cr-Mo-C-B and Fe-Cr-(Ln,Y)-Mo-C(B) and soft-magnetic (such as Fe-(Al,Ga)-(P,B,C,Si) and Fe-TM (TM - Co, Zr, Nb, Ta, W)-B [7, 8, 9].

To predict the relatively easy, different alloy systems to form glassy materials, many of indicators of glass forming ability (GFA) have been evolved. Characteristic temperature, such as liquidious temperature (T_l), glass transition temperature (T_g) and crystallisation temperature (T_x) include these indicators. Table 1 presents characteristic temperature based on GFA indicators [10, 11, 12].

Unique properties of bulk metallic glasses cause that this types of a new class of materials are used in many fields of applications (Table 2). In the near future they will be more significant than engineering materials [13, 14, 15, 16].

Table 2.
Properties and application fields of bulk metallic glasses [1, 14, 16]

No	Properties	Fields of application
1	High strength	Machinery materials
2	High hardness	Cutting materials
3	High impact fracture energy	Tool materials
4	High fatigue strength	Bonding materials
5	High fracture toughness	Die materials
6	High elastic energy	Sporting goods materials
7	Good soft magnetism	Soft magnetic materials
8	High corrosion resistance	Corrosion resistant materials
9	High reflection ratio	Optical materials
10	Efficient electrode	Electrode materials

2. Material and research methodology

Ingots of nominal content $Fe_{36}Co_{36}B_{19.2}Si_{4.8}Nb_4$, $Fe_{37}Co_{25}Ni_{10}B_{19.2}Si_{4.8}Nb_4$ and $Fe_{37}Co_{20}Ni_{15}B_{19.2}Si_{4.8}Nb_4$ were prepared by induction, melting the mixtures of Fe, Co, B, Si, Nb and Ni high purity elements in a ceramic crucible under argon atmosphere.

Bulk amorphous samples in a form of rods with diameter 2, 3, 4 and 5 mm were prepared by pressure die casting (Fig. 2). The ingots (master alloy) was melted in a quartz crucible using an induction coil and pushed into a water-cooled copper mould under pressure (Fig. 3).

Structure analysis of studied materials was carried out using X-ray diffraction (XRD). Seifert-FPM XRD 7 diffractometer with $Co_{K\alpha}$ radiation was used for all samples.

The fracture morphology of glassy materials in the form of rods with diameter of 2, 3, 4 and 5 mm was analyzed using the scanning electron microscopy (SEM) at different magnifications.

Microhardness of amorphous rods with diameter 2 and 3 mm was measured with the use of the Vickers hardness tester PMT-3 under the load of 1.962 N. Microhardness was measured on metallographic specimens of rods according to pattern presented on Figure 4: a) for rods with diameter 2 mm; b) for rods with diameter 3 mm.

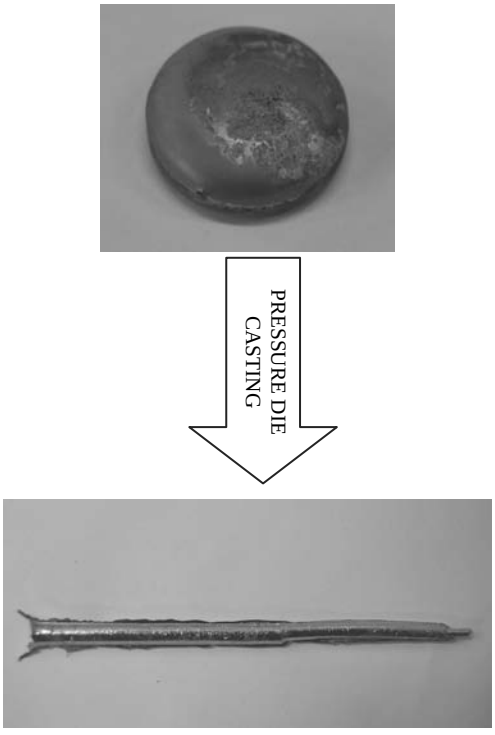

Fig. 2. Master alloy and bulk metallic glasses in a form of a rod obtained by pressure die-casting

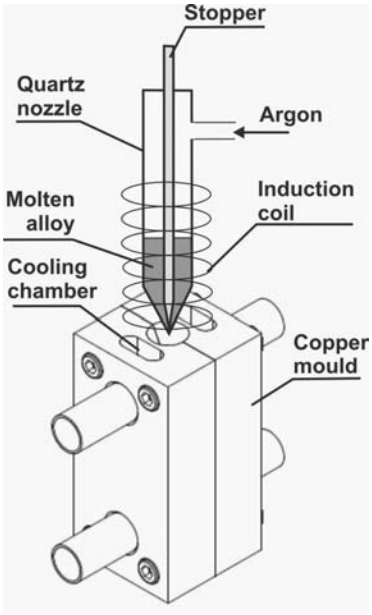

Fig. 3. Schematic illustration of the pressure die casting equipment used for casting bulk amorphous samples

a)

b)

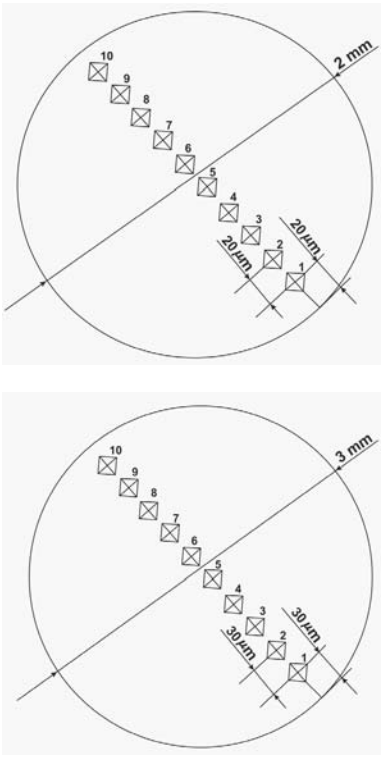

Fig. 4. The pattern of microhardness measurements: a) for rods with diameter 2 mm; b) for rods with diameter 3 mm

3. Results and discussion

From X-ray diffraction it was found that all of as-cast rods contain amorphous phase. Phase composition depends on diameter and chemical composition of alloys, especially modification of Ni and Co content.

The X-ray tests proved that the structure of die-casting rods with diameter 2 mm as well as $Fe_{36}Co_{36}B_{19.2}Si_{4.8}Nb_4$, $Fe_{37}Co_{25}Ni_{10}B_{19.2}Si_{4.8}Nb_4$ and $Fe_{37}Co_{20}Ni_{15}B_{19,2}Si_{4,8}Nb_4$ is amorphous. The growth of diameter to 3 mm caused the appearance of few crystalline phases in specimen of $Fe_{37}Co_{25}Ni_{10}B_{19.2}Si_{4.8}Nb_4$ alloy. For $Fe_{36}Co_{36}B_{19.2}Si_{4.8}Nb_4$ and $Fe_{37}Co_{20}Ni_{15}B_{19.2}Si_{4.8}Nb_4$ structure of die-casting rods with diameter 3 mm is amorphous. Structure of cast rods with diameter 4 and 5 mm is partially crystalline for all specimens. According to references 4 and 9 the best glass forming ability for Fe-Co metallic glasses reaches 4 mm. In this paper, maximum GFA came 3 mm. By the reason of modification Ni and Co percentage contents, and little change of Fe content, GFA may be changed for the worse. Good glass forming ability is also affected by fabrication conditions.

The X-ray diffraction patterns of tested rod samples are presented in Figures 5-7.

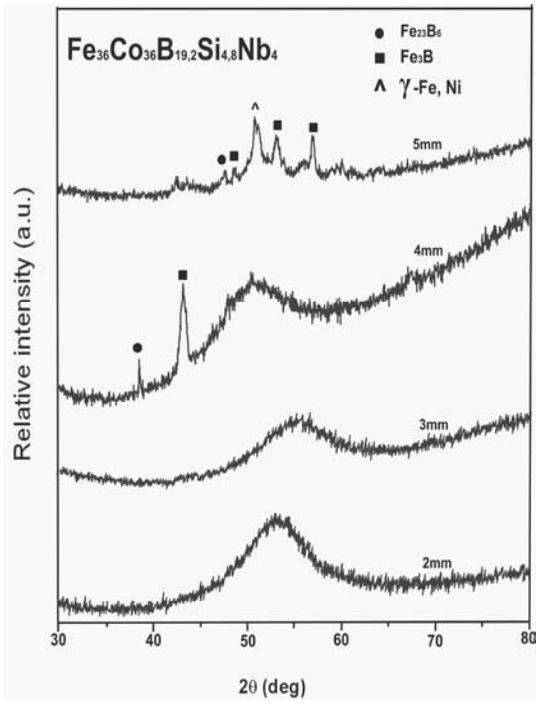

Fig. 5. X-ray diffraction patterns of the $Fe_{36}Co_{36}B_{19.2}Si_{4.8}Nb_4$ glassy rods in as-cast state with diameter 2, 3, 4 and 5 mm

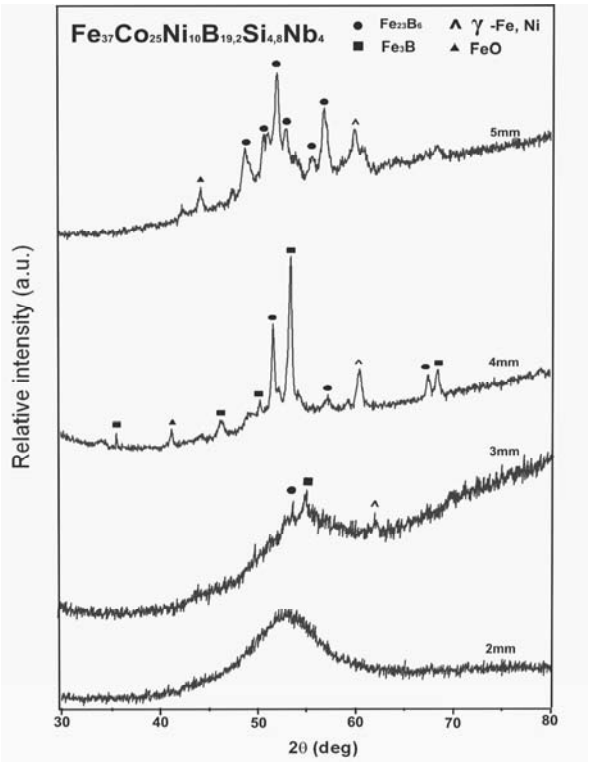

Fig. 6. X-ray diffraction patterns of the $Fe_{37}Co_{25}Ni_{10}B_{19.2}Si_{4.8}Nb_4$ glassy rods in as-cast state with diameter 2, 3, 4 and 5 mm

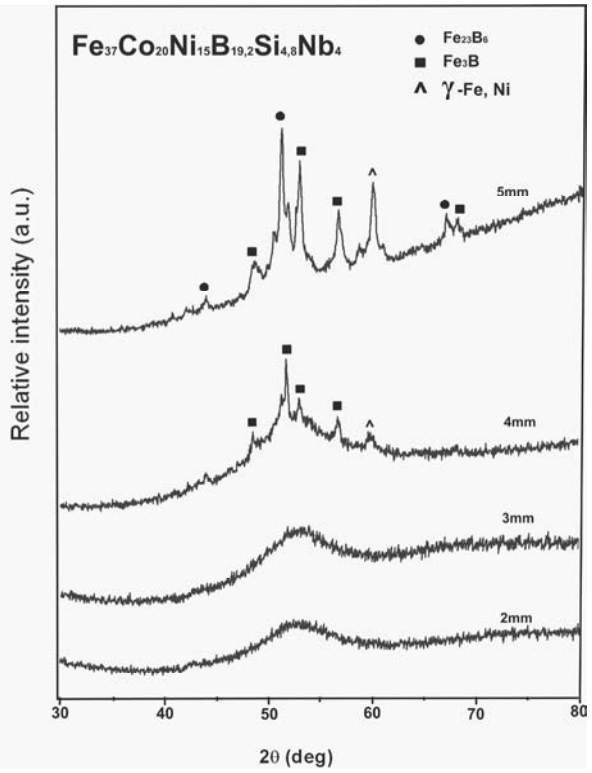

Fig. 7. X-ray diffraction patterns of the $Fe_{37}Co_{20}Ni_{15}B_{19.2}Si_{4.8}Nb_4$ glassy rods in as-cast state with diameter 2, 3, 4 and 5 mm

Microhardness testing (H_V) was realized for samples of every alloy with diameter 2 and 3 mm. Tables 3-5 presents results of microhardness experiments. The highest hardness exhibit a sample of $Fe_{37}Co_{25}Ni_{10}B_{19,2}Si_{4,8}Nb_4$ alloy with diameter 3 mm. Microhardness for this sample hesitates between 1254 H_V and 1716 H_V. For the sample $Fe_{37}Co_{20}Ni_{15}B_{19,2}Si_{4,8}Nb_4$ alloy microhardness varies between 849 and 1211 H_V for diameter 2 mm and 874 - 1299 H_V for diameter 3mm.

The Figures 8-10 present distributions of microhardness results depending on distance from surface. For $Fe_{36}Co_{36}B_{19.2}Si_{4.8}Nb_4$ alloy with diameter 2 mm microhardness value range from 956 to 1254 H_V but for diameter 3 mm it hesitates between 1027 and 1396 H_V. The lowest microhardness revealed a sample of $Fe_{37}Co_{20}Ni_{15}B_{19.2}Si_{4.8}Nb_4$ alloy with the diameter 2 mm.

Figure 11 presents SEM micrographs of as-cast glassy rod with diameter 2 mm of $Fe_{36}Co_{36}B_{19.2}Si_{4.8}Nb_4$ alloy, Figure 12 shows micrographs of as-cast glassy rod with diameter 3, of the same alloy. Figure 13 shows micrographs of as-cast glassy rod with diameter 2 mm of $Fe_{37}Co_{25}Ni_{10}B_{19.2}Si_{4.8}Nb_4$ alloy, Figure 14 present micrographs of as-cast glassy rod with diameter 3 mm of the same alloy. Final Figure 15 show micrographs of as-cast glassy rod with diameter 3 mm of $Fe_{37}Co_{20}Ni_{15}B_{19.2}Si_{4.8}Nb_4$ alloy.

The fracture testing was realized in few areas which are marked as A, B or C. The presented fractures could be classified as mixed fracture: smooth, partially shell and veinlet.

On the basis of SEM micrographs, it was found that morphology changes from smooth on the margin of samples where surface had contact with copper mould during casting, to shell and veinlet in the centre.

Table 3.
Results of microhardness experiments of $Fe_{36}Co_{36}B_{19.2}Si_{4.8}Nb_4$ rods with diameter 2 and 3 mm

No.	$Fe_{36}Co_{36}B_{19.2}Si_{4.8}Nb_4$ with diameter 2 mm			$Fe_{36}Co_{36}B_{19.2}Si_{4.8}Nb_4$ with diameter 3 mm		
	Distance between stamps [μm]	Distance from margin [μm]	H_V	Distance between stamps [μm]	Distance from margin [μm]	H_V
1	---------	20	1049	---------	20	1095
2	20	40	1211	30	50	1254
3	20	60	1171	30	80	1120
4	20	80	956	30	110	1171
5	20	100	1132	30	140	1299
6	20	120	1211	30	170	1254
7	20	140	1095	30	200	1211
8	20	160	956	30	230	1132
9	20	180	1254	30	260	1027
10	20	190	1195	30	290	1396

Table 4.
Results of microhardness experiments of $Fe_{37}Co_{25}Ni_{10}B_{19.2}Si_{4.8}Nb_4$ rods with diameter 2 and 3 mm

No.	$Fe_{37}Co_{25}Ni_{10}B_{19.2}Si_{4.8}Nb_4$ with diameter 2 mm			$Fe_{37}Co_{25}Ni_{10}B_{19.2}Si_{4.8}Nb_4$ with diameter 3 mm		
	Distance between stamps [μm]	Distance from margin [μm]	H_V	Distance between stamps [μm]	Distance from margin [μm]	H_V
1	---------	20	1049	---------	20	1254
2	20	40	1095	30	50	1716
3	20	60	927	30	80	1584
4	20	80	985	30	110	1716
5	20	100	1017	30	140	1254
6	20	120	1171	30	170	1716
7	20	140	927	30	200	1396
8	20	160	956	30	230	1254
9	20	180	1049	30	260	1254
10	20	190	1254	30	290	1524

Table 5.
Results of microhardness experiments of $Fe_{37}Co_{20}Ni_{15}B_{19.2}Si_{4.8}Nb_4$ rods with diameter 2 and 3 mm

No.	$Fe_{37}Co_{20}Ni_{15}B_{19.2}Si_{4.8}Nb_4$ with diameter 2 mm			$Fe_{37}Co_{20}Ni_{15}B_{19.2}Si_{4.8}Nb_4$ with diameter 3 mm		
	Distance between stamps [μm]	Distance from margin [μm]	H_V	Distance between stamps [μm]	Distance from margin [μm]	H_V
1	---------	20	985	---------	20	1211
2	20	40	1017	30	50	1211
3	20	60	849	30	80	985
4	20	80	1171	30	110	1299
5	20	100	1211	30	140	1346
6	20	120	1171	30	170	985
7	20	140	1120	30	200	1095
8	20	160	1049	30	230	874
9	20	180	1120	30	260	956
10	20	190	1132	30	290	1049

a) b)

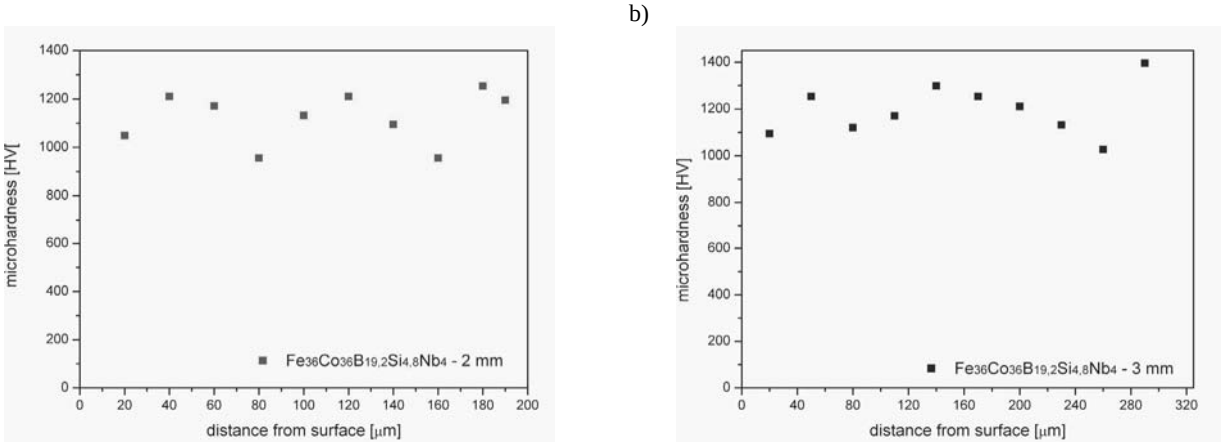

Fig. 8. Microhardness results distribution for amorphous rods of $Fe_{36}Co_{36}B_{19.2}Si_{4.8}Nb_4$ alloy with diameter 2 mm (a) and 3 mm (b)

a) b)

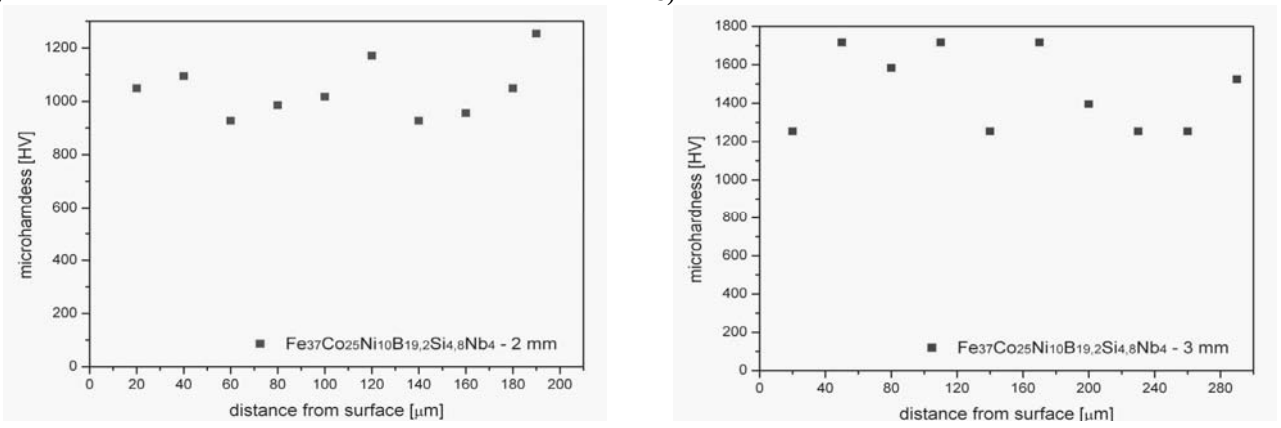

Fig. 9. Microhardness results distribution for amorphous rods of $Fe_{37}Co_{25}Ni_{10}B_{19.2}Si_{4.8}Nb_4$ alloy with diameter 2 mm (a) and 3 mm (b)

a) b)

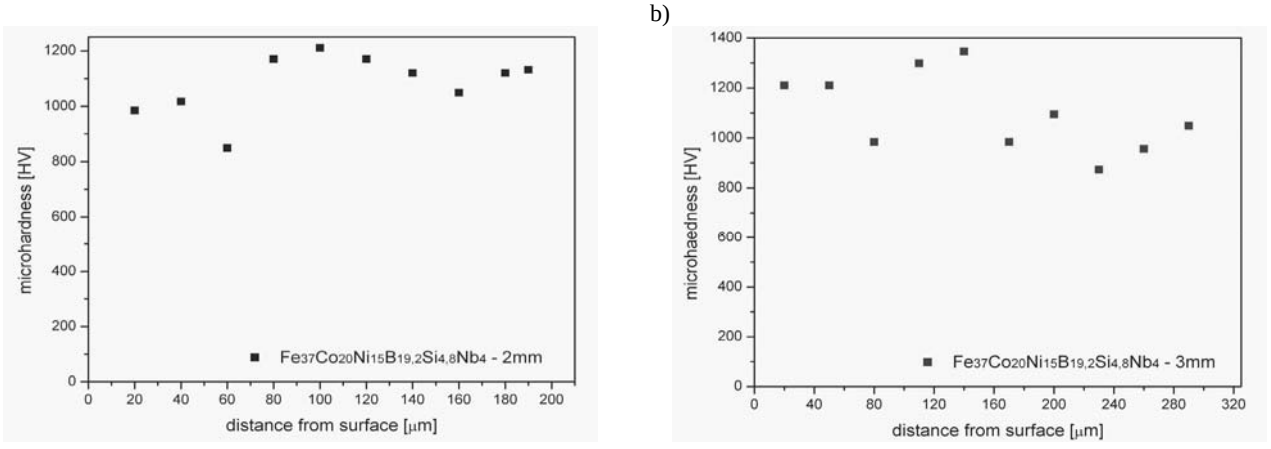

Fig. 10. Microhardness results distribution for amorphous rods from $Fe_{37}Co_{20}Ni_{15}B_{19.2}Si_{4.8}Nb_4$ alloy with diameter 2 mm (a) and 3 mm (b)

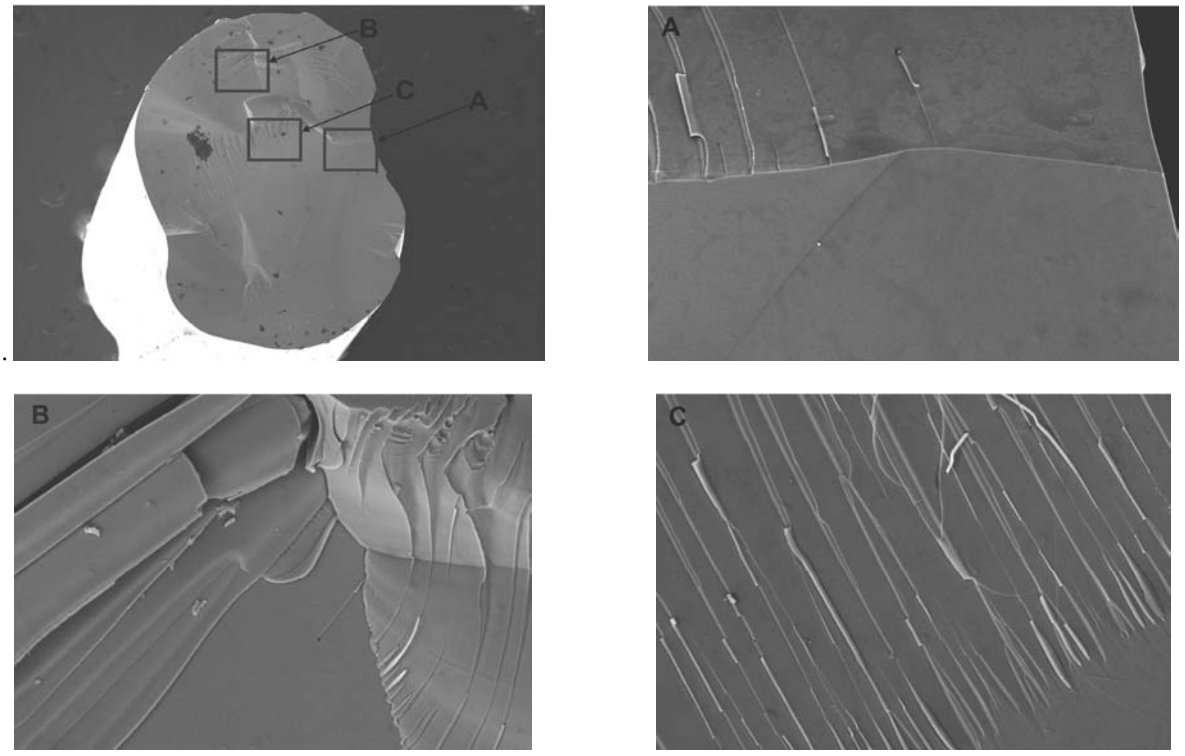

Fig. 11. SEM micrograph of the fracture morphology of as-cast rod of $Fe_{36}Co_{36}B_{19.2}Si_{4.8}Nb_4$ alloy with diameter 2 mm; (A-rod's core; B- zone between a core and a rod margin)

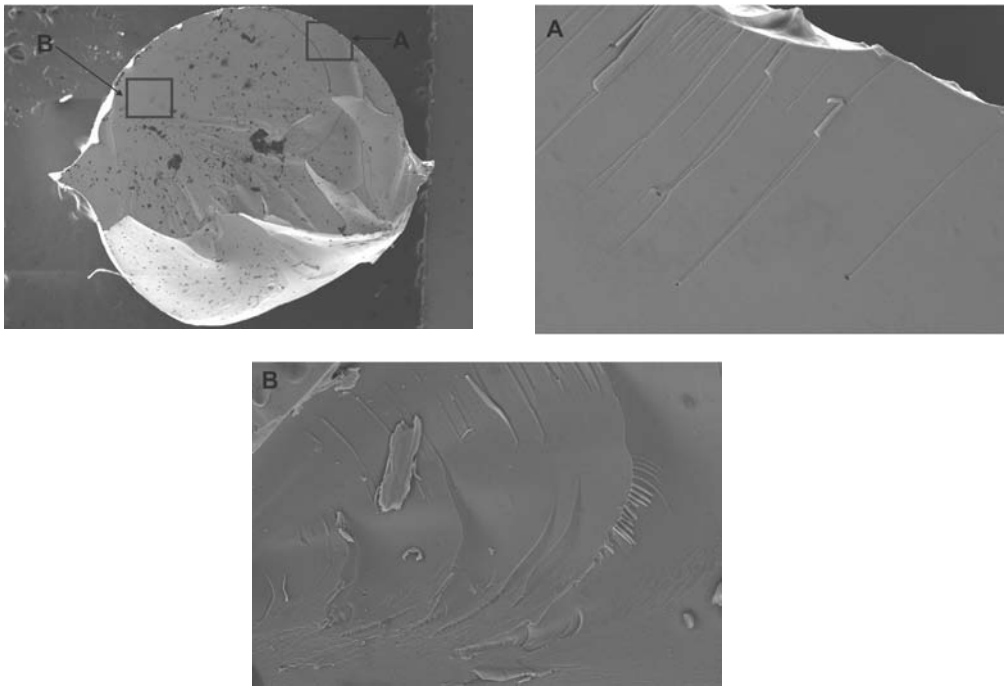

Fig. 12. SEM micrograph of the fracture morphology of as-cast rod of $Fe_{36}Co_{36}B_{19.2}Si_{4.8}Nb_4$ alloy with diameter 3 mm; (A-margin of sample; B- zone between a core and a rod margin)

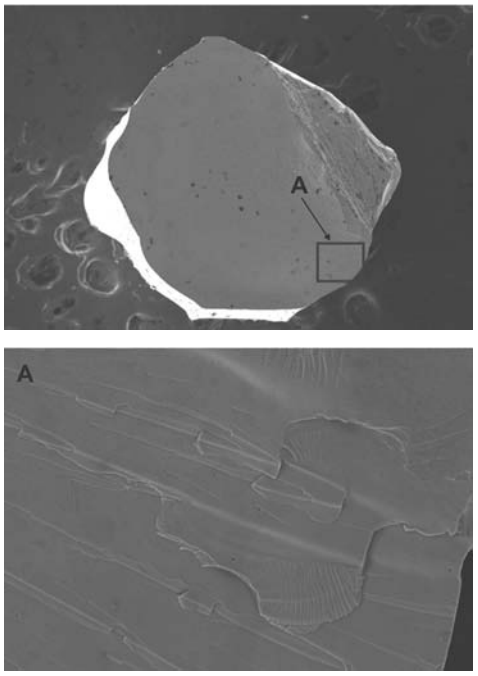

Fig. 13. SEM micrograph of the fracture morphology of as-cast rod of $Fe_{37}Co_{25}Ni_{10}B_{19.2}Si_{4.8}Nb_4$ alloy with diameter 2 mm; (A- margin of the sample)

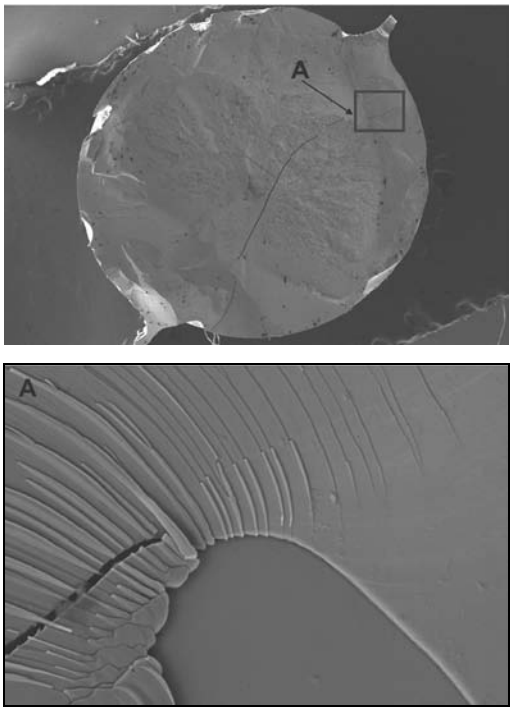

Fig. 14. SEM micrograph of the fracture morphology of as-cast rod of $Fe_{37}Co_{25}Ni_{10}B_{19.2}Si_{4.8}Nb_4$ alloy with diameter 3 mm; (A- zone between a core and a rod margin)

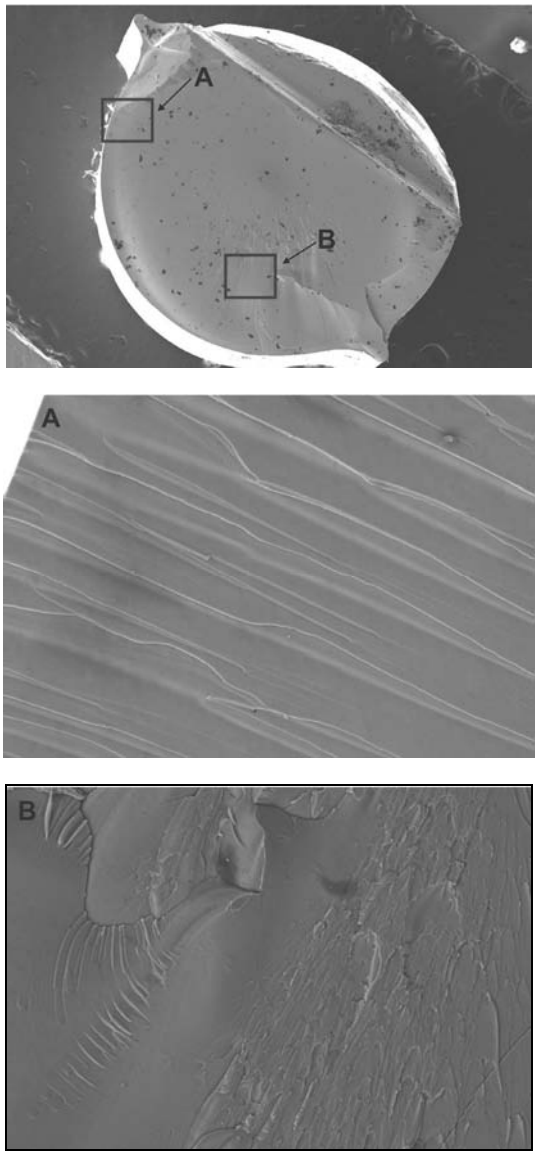

Fig. 15. SEM micrograph of the fracture morphology of as-cast rod of $Fe_{37}Co_{20}Ni_{15}B_{19.2}Si_{4.8}Nb_4$ alloy with diameter 3 mm; (A- margin of the sample; B- zone between a core and a rod margin)

4. Conclusions

The investigations which were performed on the samples of the $Fe_{36}Co_{36}B_{19.2}Si_{4.8}Nb_4$, $Fe_{37}Co_{25}Ni_{10}B_{19.2}Si_{4.8}Nb_4$ and $Fe_{37}Co_{20}Ni_{15}B_{19.2}Si_{4.8}Nb_4$ bulk metallic glasses allow to formulate the following conclusions:

- The X-ray diffraction confirmed that as-cast bulk samples with diameter 2 and 3 mm exhibit amorphous structure. Rod with 3 mm diameter $Fe_{37}Co_{25}Ni_{10}B_{19.2}Si_{4.8}Nb_4$ reveal some crystalline phases;

- All as-cast bulk samples with diameter 4 and 5 mm reveal crystalline phases in their structure;
- Addition of nickel and modification of Co amount in $Fe_{36}Co_{36}B_{19.2}Si_{4.8}Nb_4$ alloy had an influence on its glass forming ability;
- The sample's structure depends on its diameter and chemical composition;
- Addition of nickel in 10 and 15 at% amount caused appearance of crystalline phases in rods with diameter 3 mm;
- Growth of the sample's diameter as a result of revealed crystalline phases in all samples;
- The highest microhardnes exhibits a sample with diameter 3mm of $Fe_{37}Co_{25}Ni_{10}B_{19.2}Si_{4.8}Nb_4$ alloy; The lowest microhardness reveals glassy rod of $Fe_{37}Co_{20}Ni_{15}B_{19.2}Si_{4.8}Nb_4$ alloy with the diameter 2 mm;
- Amorphous samples exhibit smooth fracture on the margin where surface had contact with copper mould during casting, and shell or veinlet in the centre;
- The present Fe-based metallic glasses with good GFA and hardness may be promising engineering materials for many important applications (e.g. cores of transformers).

Acknowledgements

This work was supported by Polish Ministry of Science under grant No. 0661/T02/2006/31.

References

[1] M. Telford, The case for bulk metallic glass, Materials Today March 2004 (2004) 36-43.
[2] B. Shen, C. Chang, A. Inoue, Formation, ductile deformation behaviour and soft – magnetic properties of (Fe, Co, Ni)-B-Si-Nb bulk glassy alloys, Intermetallics 15 (2007) 9-16.
[3] R. Nowosielski, R. Babilas, Fabrication of bulk metallic glasses by centrifugal casting method, Journal of Achievements in Materials and Manufacturing Engineering 20 (2007) 487-490.
[4] A. Inoue, Bulk amorphous and nanocrystalline alloys with high functional properties, Materials Science and Engineering A 304-306 (2001) 1-10.
[5] S.F. Guo, L. Liu, N. Li,Y. Li, Fe-based bulk metallic glass matrix composite with large plasticity, Scripta Materialia 62 (2010) 329-332.
[6] K.J. Laws, B. Gun, M. Ferry, Effect of die-casting parameters on the production of high quality bulk metallic glasses samples, Materials Science and Engineering A 425 (2006) 114-120.
[7] S. Lesz, P. Kwapuliński, R. Nowosielski, Formation and physical properties of Fe-based bulk metallic glasses with Ni addition, Journal of Achievements in Materials and Manufacturing Engineering 31/1 (2008) 35-40.
[8] W.H. Wang, Roles of minor additions in formation and properties of bulk metallic glasses, Progress in Materials Science 52 (2007) 540-596.
[9] A. Inoue, B.L. Shen, C.T. Chang, Fe- and Co-based bulk glassy alloys with ultrahigh strength of over 4000 MPa, Intermetallics 14 (2006) 934-944.
[10] V. Jindal, V.C. Srivastava, V. Uhlenwinkel, On the role of liquid phase stability and GFA parameters, Journal of Non-Crystalline Solids 335 (2009) 1552-1555.
[11] A. Suryanarayana, I. Seki, A. Inoue, A critical analysis of the glass-forming ability of alloys Journal of Non-Crystalline Solids 355 (2008) 355-360.
[12] R. Nowosielski, A. Witrak, Formation and structure of $Co_{50}Cr_{15}Mo_{14}C_{15}B_6$ bulk metallic glasses, Archives of Materials Science and Engineering 36/1 (2009) 28-33.
[13] S.S Wua, B. Shenb, A. Inoue, Preparation and properties study of bulk $Fe_{75.5}Ga_3P_{10.5}C_4B_4Si_3$ metallic glass ring by copper mould casting, Intermetallics 12 (2004) 1261-1264.
[14] R. Nowosielski, R. Babilas, Structure and magnetic properties of $Fe_{36}Co_{36}B_{19}Si_5Nb_4$ bulk metallic glasses, Proceedings of the 12th International Materials Symposium, IMSP'2008, Denizli, Turkey, 2008, 101-106.
[15] P. Kwapuliński, J. Rasek, Z. Stokłosa, G. Badura, B. Kostrubiec, G. Haneczok, Magnetic and mechanical properties in FeXSiB (X=Cu, Zr, Co) amorphous alloy, Archives of Materials Science and Engineering 31/1 (2008) 25-28.
[16] L.A. Dobrzański, M. Drak, B. Ziębowicz, Materials with specific magnetic properties, Journal of Achievements in Materials and Manufacturing Engineering 17 (2006) 37-40.